

Localized states and the electronic properties of a hydrogenated defect in amorphous silicon

D. P. DiVincenzo

Department of Electrical Engineering and Department of Physics, University of Pennsylvania, Philadelphia, Pennsylvania 19104

J. Bernholc

Corporate Research Science Laboratories, Exxon Research and Engineering Company, Linden, New Jersey 07036

M. H. Brodsky

IBM Thomas J. Watson Research Center, Yorktown Heights, New York 10598

(Received 13 April 1983)

We study the electronic properties of a hydrogen-dressed silicon monovacancy as a model of H centers in hydrogenated amorphous silicon (*a*-Si:H). Using the self-consistent Green's-function technique, we obtain total and local densities of states for the defect, as well as the charge density of defect eigenstates. The hydrogenated vacancy has no states in the band gap and reduces the Si host density of states at both the valence- and conduction-band edge. The Si-H bonding character of the defect eigenstates is greatest 4.5 eV below the valence-band edge; however, no sharp H-induced resonance occurs anywhere in the valence or conduction bands. We discuss the importance of including the self-consistent rearrangement of charge around the H atom in obtaining accurate results for the hydrogenated vacancy. Within the context of a recently proposed quantum-well model, we relate the results of our Green's-function calculation to the properties of *a*-Si:H. Using several simple models (percolation theory, the Anderson model, effective-mass theory), we obtain estimates for the valence- and conduction-band mobility edges. We find that the valence band is much more strongly affected than the conduction band by H disorder, and that H disorder is more important than dihedral-angle disorder in valence-band edge localization.

I. INTRODUCTION

In recent years there has been considerable interest in the electronic properties of hydrogenated amorphous silicon (*a*-Si:H),¹ in part because of its technological promise and in part because it is a prototype semiconductor for the study of the amorphous state. Of particular importance is that *a*-Si:H can be doped by the same dopants used for crystalline Si; further, its room-temperature photoconductivity and low-temperature photoluminescence are high, its absorption coefficient is well matched to the solar spectrum in the visible, and junction devices have been successfully formed with it. Hydrogen plays a fundamental, but not thoroughly understood role in modifying the properties of pure amorphous Si (*a*-Si). The simplest chemical model which accounts for the strength of the Si-H bond gives a qualitative account of the reduction of band-gap states due to dangling bonds, and of the increase in the average band gap compared with *a*-Si. Many of the experiments on *a*-Si:H, however, still lack quantitative explanation. Photoemission, optical-absorption, and transport experiments provide evidence for significant modifications caused by hydrogen of both the valence- and conduction-band states of the material. The understanding of these observations requires as a start a detailed microscopic, quantum-mechanical description of the electronic properties of Si-H bonds in a Si host environment.

The present work provides such a description.² We have calculated in detail the electronic spectrum and the physical charge configuration of a single isolated H-

saturated monovacancy in crystal Si (*x*-Si). Since this model simply consists of four Si-H units pointing into a small void, it permits the study of H-induced disorder in Si exclusive of other disordering effects in *a*-Si (e.g., bond distortions, dihedral-angle variations, broken bonds, impurities, odd-membered rings, etc.). To the extent that the four Si-H units within the vacancy in this model are decoupled (our calculation indicates only a small coupling), our work also gives information about the isolated Si-H bond itself, which is known to be one of the constituents of *a*-Si:H. The model defect's high symmetry was chosen so that a recently developed self-consistent Green's-function technique³ could be applied to it. This technique has been proven to give accurate results for the bare vacancy in *x*-Si, as well as in a variety of other point defects. Most important, the use of atomically derived ionic pseudopotentials permits the detailed examination of the charge density of the Si-H bond and surrounding Si-Si bonds; these results are helpful in interpreting the significance of changes in the electronic density of states caused by H.

The results of our work are consistent with the view that H is responsible for a local expansion of the band gap in *a*-Si:H as compared with pure *a*-Si. State density is reduced at both the valence- and conduction-band edge, with the greater effect on the valence band. No gap states are induced by the presence of H. Detailed study of the valence band shows that the charge density of states deep in the valence band is increased on the Si-H bond, with the largest enhancement about -4.5 eV below the band

gap. However, there is no indication of a sharp H resonance at this energy or at any other energy studied. Near the valence-band edge, the presence of H is found to have a large, long-ranged effect on the eigenstates with a significant influence at least 4 Å from the defect; this effect is not seen at any other energy in the valence band. For states at the conduction-band edge, the defect causes a somewhat more complicated disturbance. Eigenstate amplitudes are reduced near the removed Si site and increased near the added Si-H bonds; this could be the analog of the H resonance seen in other calculations^{4,5} near the conduction-band edge. However, the present calculation indicates that this conduction-band disturbance is not a genuine resonance, and the total density of states is actually slightly reduced at the band edge by the defect.

The details of the modification of band-edge states take on particular importance within the context of a quantum-well model which has recently been proposed⁶ to explain a wide range of optical-absorption and electrical-transport data on *a*-Si:H. The quantum-well model makes certain assumptions about the electronic properties of the Si-H bond which we test in the present work. The key conjecture of the model is that regions of potential emanating from Si-H bonds form barriers that confine low-energy electrons and holes to islands of pure Si simply because of the presence of bonded H. The model assumes that the energies of both the local conduction- and valence-band edges in the Si-H region are, respectively, larger and smaller than the delimiting conduction- and valence-band energies of the pure-Si band gap. The zero-point energy of confinement of carriers in these "quantum wells" accounts for the increased energies of photoluminescence and optical absorption with respect to the gap of crystal Si, while the residual height of the Si-H barriers (after allowance for interwell tunnelling) determines the activation energy for conduction, and provides the aperiodic disturbances that help to induce the extra strength of the optical-absorption edge. The model requires that the sum of the band-edge shifts in the H-rich regions be several eV, and that these enlarged local gaps extend away from the Si-H regions into the Si islands by about one bond length. The results of the present calculation lend qualitative, and to some extent quantitative, support to these assumptions and requirements of the quantum-well model. In addition to these correspondences, the present work used percolation theory, the Anderson localization model, and a simplified effective-mass theory to note some connections between H disorder in *a*-Si:H and localized band-edge states.

As intensive study in recent years has shown, *a*-Si:H is a complex material whose properties have not yet been explained simply from any single point of view. This is reflected by the large number of different theoretical approaches which have been used to describe it. Most akin to the present work is that of Papaconstantopoulos and Economou⁴ who studied the properties of the same model hydrogenated vacancy. With the use of a simpler tight-binding Hamiltonian, a coherent potential approximation permitted them to consider the average electronic structure of the H-disordered material. A companion work by Pickett⁵ examined the electronic structure of hydrogenated

defects in a periodic supercell. Another approach to the Si-H defect has been taken by Allan and Joannopoulos⁷ who have obtained the electronic spectrum and total energy of a number of different hydrogen sites (Si-H, Si-H₂, H-Si-Si-H, etc.) within a Bethe-lattice model. The work of Johnson *et al.*⁸ and by Ching *et al.*⁹ has studied finite-cluster models of different Si-H configurations.

This paper is organized as follows: Sec. II describes the physical Si-H configuration to be studied, Sec. III outlines the self-consistent Green's-function formalism, Sec. IV presents the results of the Green's-function calculation, Sec. V relates the results of the defect calculation to the properties of *a*-Si:H, and Sec. VI gives our conclusions.

II. MODEL

As Fig. 1 shows, our model defect is formed by removing a single Si atom from the perfect Si crystal and replacing it by four H atoms placed 1.48 Å from each of the four nearest-neighbor Si atoms. Although no direct measurement of the bond length in *a*-Si:H exists, the similarity of the Si-H distance in several different chemical environments¹⁰ argues for the transferability of this length. Neither relaxation of the Si-H bond nor of the surrounding Si-Si bonds will be considered here. The results of our calculation suggest that if any relaxation actually occurs, it is small. Because there are no gap states, none of the Jahn-Teller effects seen in nonhydrogenated vacancies are predicted. Therefore, the covalent bonding for atoms neighboring the defect site is rather undisturbed. In the geometry considered here, H atoms are separated by 1.4 Å. Although this means that the H-H distance in this configuration is smaller than the Si-H distance, the H's are separated by twice their molecular bond length, 0.7 Å. The present calculation indicates that an H-H interaction exists in this model, but that it is much smaller than other interactions in the problem.

We have modeled both the Si and H atoms with local pseudopotentials. The Si pseudopotential is identical to that used in a previous calculation of the electronic structure of the bare Si monovacancy.³ The H ionic pseudopotential (in Ry) has been modeled by the analytic form

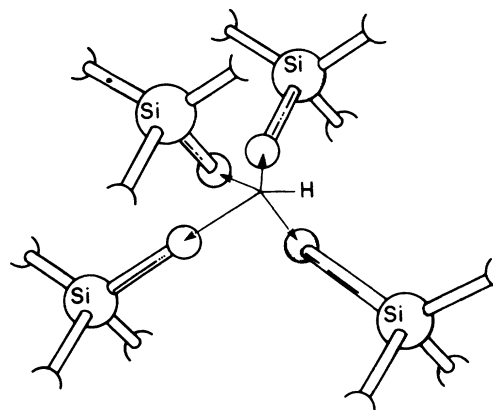


FIG. 1. Fully saturated H monovacancy in *x*-Si. Si-Si bond length is 2.35 Å, Si-H bond length is 1.48 Å, and distance between H atoms is 1.4 Å.

$$V(r) = -\frac{2Z}{r} \operatorname{erf}\left[\frac{r}{r_c}\right] + \frac{\alpha}{r_c} e^{-r^2/r_c^2}, \quad (1)$$

with $\alpha = -1.6$ a.u., proton charge $Z = 1$, and $r_c = 0.7$ a.u. This potential accurately reproduces both the $1s$ eigenenergy and wave function of the isolated H atom.

III. CALCULATION

The electronic structure of our model defect has been calculated with the self-consistent Green's-function method^{3,11} In operator notation, this technique may be described as follows. The perfect-crystal Green's-function operator is defined as

$$G^0(E) = \lim_{\epsilon \rightarrow 0^+} \left[\frac{1}{E - H^0 + i\epsilon} \right], \quad (2)$$

where H^0 is the Hamiltonian of the perfect crystal. If the Hamiltonian of the system containing the point defect is separated into $H = H^0 + V$, then the total Green's-function operator is given by

$$G(E) = [1 - G^0(E)V]^{-1}G^0(E). \quad (3)$$

The position of the bound states within the band gap is given by the condition

$$D(E) = \det[\mathbf{1} - \underline{G}^0(E)\underline{V}] = 0, \quad (4)$$

while the defect-induced change in the density of states $N(E)$ is given by

$$\Delta N(E) = \frac{2}{\pi} \frac{d\delta(E)}{dE} \quad (5)$$

(spin included), where the phase shift $\delta(E)$ is

$$\delta(E) = -\tan^{-1} \left[\frac{\operatorname{Im}D(E)}{\operatorname{Re}D(E)} \right]. \quad (6)$$

For these operator equations to be useful, they must be studied within some particular basis set. It has been verified formally^{3,12} that only a limited number of basis functions $\Phi_\alpha(\vec{r})$, namely those for which the defect-potential matrix elements $V_{\alpha\beta}$ are nonzero, are necessary to give the new density of states correctly.

Similarly, the change in the charge density in real space may also be obtained as follows:

$$\Delta\rho(\vec{r}) = \int_{-\infty}^{E_F} \sum_{\alpha,\alpha'} \Phi_\alpha^*(\vec{r}) \left[-\frac{2}{\pi} \right] \times \operatorname{Im}[G_{\alpha\alpha'}(E) - G_{\alpha\alpha'}^0(E)] \Phi_{\alpha'}(\vec{r}) dE, \quad (7)$$

where E_F is the Fermi energy.

The requirement of self-consistency has been satisfied in the following by creating a new defect potential according to the Kohn-Sham procedure¹³:

$$V(\vec{r}) = \Delta V_{\text{ion}} + \frac{e^2}{2} \int \frac{\Delta\rho(\vec{r}')}{|\vec{r} - \vec{r}'|} d\vec{r}' + V_{\text{xc}}[\rho] - V_{\text{xc}}[\rho_0], \quad (8)$$

TABLE I. Decay lengths α of Gaussian basis functions $e^{-\alpha r^2}$ (a.u.)⁻².

Si				
	<i>s</i>	<i>p</i>	<i>d</i>	<i>f</i>
α	0.3,0.7,0.14	0.25	0.25	0.25
H				
	<i>s</i>	<i>p</i>		
α	0.3,0.8,1.6	0.25		

where $\Delta\rho = \rho(\vec{r}) - \rho^0(\vec{r})$, $\rho^0(\vec{r})$ is the perfect Si charge density, and $V_{\text{xc}}[\rho]$ is the $X\alpha$ approximation to the exchange and correlation potentials with $\alpha = 0.7$. Equations (3)–(8) have been solved iteratively until the difference between output and input defect potentials $V(r)$ is less than 0.005 Ry. The effects of self-consistency on the present work have been found to be important, as will be discussed below.

For analysis of the results, we also need energy-resolved changes in the charge density,

$$\Delta\rho(E, \vec{r}) = -\frac{2}{\pi} \sum_{\alpha,\alpha'} \Psi_\alpha^*(\vec{r}) \operatorname{Im}[G_{\alpha\alpha'}(E) - G_{\alpha\alpha'}^0(E)] \Phi_\alpha(\vec{r}). \quad (9)$$

Since the spatial extent of $\Delta\rho(E, \vec{r})$ is much greater than that of $V(r)$ and $\Delta\rho(r)$, we have chosen a rather extensive set of basis functions which extends well beyond the second-nearest neighbors of the defect. Specifically, the basis functions $\Phi(\vec{r})$ have been taken to be localized Gaussians $e^{-\alpha r^2}$ multiplied by real spherical harmonics centered on the atomic sites in the vicinity of the defect. The Si basis functions include three *s*-like Gaussians with decay constants $\alpha = 0.3, 0.7, \text{ and } 1.4$ a.u., three *p*-like Gaussians all with decay constant $\alpha = 0.25$ a.u., five *d*-like Gaussians with decay constant $\alpha = 0.25$ a.u., and one *f*-like Gaussian (xyz) with decay constant $\alpha = 0.25$ a.u. These basis functions are placed on the missing Si site at the center of monovacancy, on the four nearest-neighbor Si atoms, and on the twelve next-nearest-neighbor Si atoms. The H-centered orbitals include three *s*-like Gaussians with $\alpha = 0.3, 0.8, \text{ and } 1.6$ a.u., and three *p*-like Gaussians with $\alpha = 0.25$ a.u. A summary of the basis set is given in Table I.

IV. RESULTS

Using the technique described above, we have calculated the following quantities for the fully hydrogenated defect: The difference $\Delta N(E)$ between the defect density of states and the pure *x*-Si density of states, the total charge density $\rho(\vec{r})$, the difference charge density $\Delta\rho(\vec{r})$ for eigenstates near the Si valence- and conduction-band edges and inside the valence band, and the local density of states for several bond regions in the vicinity of the hydrogenated vacancy, e.g., the Si–H bond and the neighboring Si–Si bond. We present and describe in detail each of these results below.

Figure 2 shows the total density of states $N^0(E)$ for *x*-Si

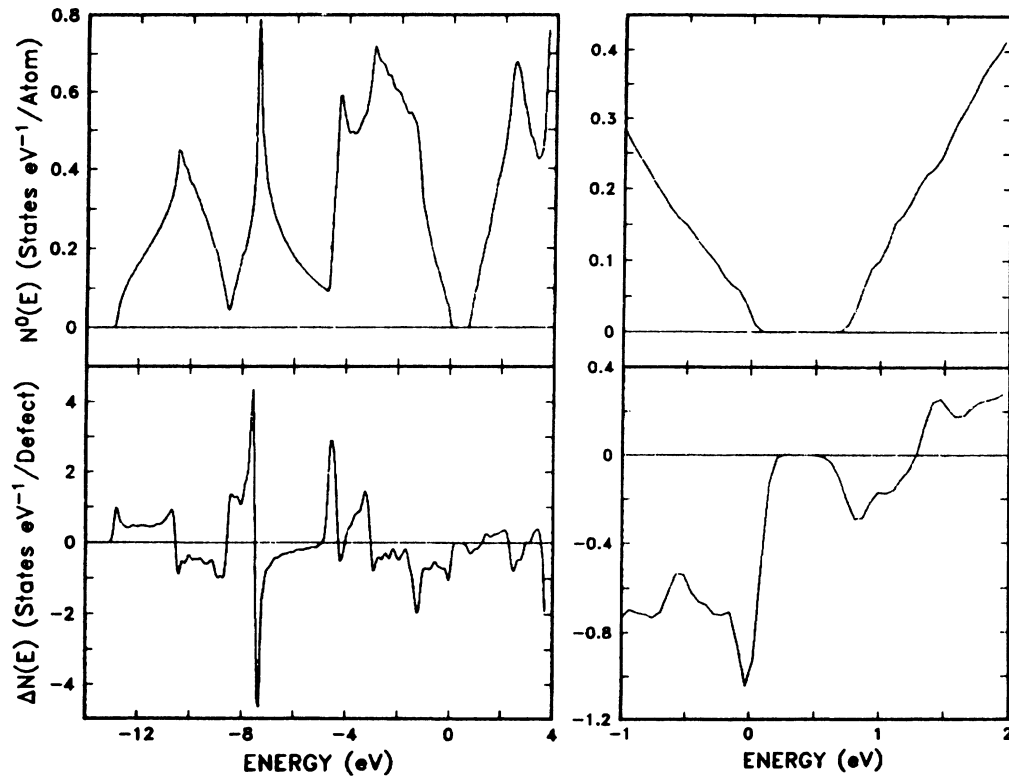


FIG. 2. Pure x -Si density of states $N^0(E)$ and the change $\Delta N(E)$ induced by a single hydrogenated defect. Left-hand panels show entire valence band and first 3 eV of conduction band; right-hand panels focus on the vicinity of the band gap.

and the difference $\Delta N(E)$ between the density of states of an infinite crystal with one defect and the perfect system. The defect produces no bound states either in the Si band gap or below the bottom of the valence band, so the changes occur only inside the valence and conduction bands as shown. The principal effect of the defect on the valence band is to shift essentially Si-like states to lower energy; the Si-H bonding character acquired by these states is weak, as we discuss below. Thus $\Delta N(E) > 0$ at the bottom of the valence band, below the Si density of states peak at -7.5 eV, and below the heavy-hole peak around -3 eV. Conversely, the $\Delta N(E)$ curve shows depletion above each $N^0(E)$ valence-band peak, and especially near the top of the valence band at 0 eV. $\Delta N(E)$ appears to tail into the gap because it contains a strong $E^{-1/2}$ singularity at the valence-band edge which has been broadened in our calculation, i.e., $\epsilon > 0$ in Eq. (2). The bottom of the conduction band also shows a small removal of density of states. Through the entire energy region shown we did not find any true resonant H-like states; there is, however, a discernible maximum in the Si-H bonding character of the vacancy eigenstates near -4.5 eV, as we will show later.

The removal of states from the band edges shown in the lower right panel of Fig. 2 has particular significance for the quantum-well model. Loosely speaking, the depletion implies that *both* electrons and holes are "repelled" from the defect site, so that the hydrogenated defect presents a barrier to band-edge carriers. The decrease in the density of states which we find at the top of the valence band is in reasonable agreement with the 0.4-eV recession of the

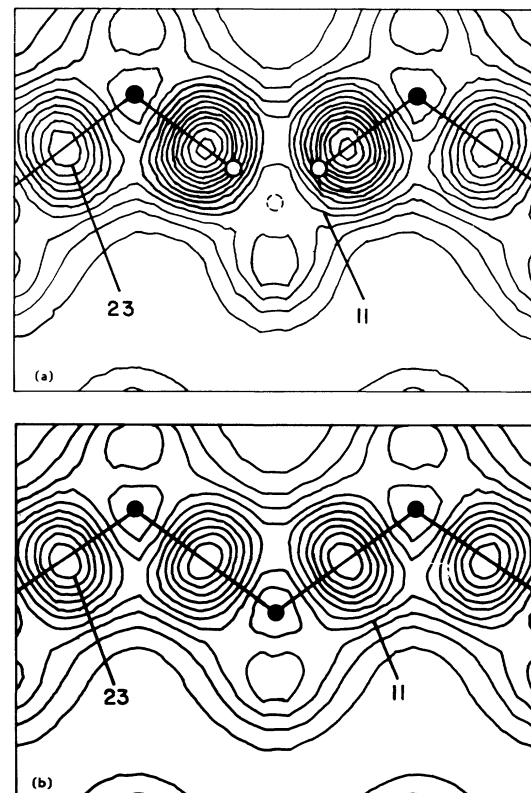


FIG. 3. (a) Valence charge density $\rho(\vec{r})$ in a (110) plane passing through the hydrogenated vacancy, (b) $\rho^0(\vec{r})$ in a (110) plane for a perfect crystal. Units are electrons/ \AA^3 . Solid circles denote Si atoms and open circles denote H atoms.

band edge found by photoemission¹⁴ and reported in previous theoretical studies^{4,5,8,9}. We also find a small recession of the conduction-band edge, while previous theories^{4,5} have shown no movement of the band edge. In general, we expect the pseudopotential Green's-function technique used in this work to be a more appropriate description of conduction-band states than previously used tight-binding or supercell calculations. We avoid the inadequate basis set of the former and the nonphysical defect periodicity of the latter. A more quantitative analysis of band-edge properties is given in the discussion.

A complementary point of view of the electronic structure of the hydrogenated vacancy is provided by the total valence charge density. Figure 3(a) shows $\rho(\vec{r})$ in a (110) plane passing through the hydrogenated vacancy. Two of the H atoms lie in this plane, one lies below and one above. The most noticeable feature of this contour plot is that the total charge density has not been substantially modified at the defect compared to that at the perfect crystal [$\rho^0(\vec{r})$; see Fig. 3(b)]. The maximum of the bond charge density remains in the same place as in the undisturbed material, and its shape remains roughly the same. It might be thought that this result may occur accidentally because of the particular symmetry of the model structure which places four protons ($Z=1$) close to the center which originally contained a (pseudo-) Si atom ($Z=4$). However, similarly shaped Si-H bonds with increased charge near the H atom have been seen in other Si-H-bonded systems (e.g., surfaces¹⁵ and vacancy supercells⁵). We believe that our calculation shows features of four essentially isolated Si-H bonds. Among these features is that the Si-H bond is noticeably more peaked than the Si-Si bond charge, indicative of the greater strength of the Si-H bonding. This effect is brought out in $\Delta\rho(\vec{r})$, the difference between the defect charge density and the pure-Si charge density prior to creation of the vacancy (Fig. 4). The figure shows that charge is removed from the interstitial regions of the defect and concentrated in the bond. It also shows that the modification of the back-bond region and of the next Si-Si region is very small. However, it is incorrect to conclude that the effects of the H defect are short ranged. Figure 5 shows the

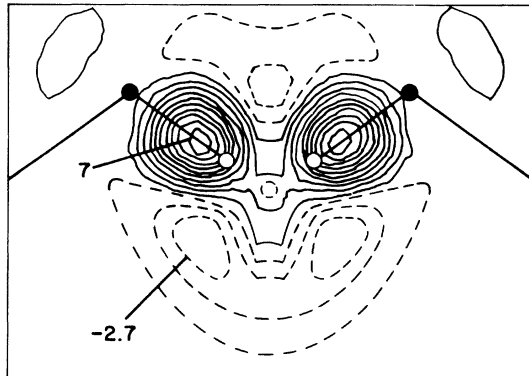


FIG. 4. $\Delta\rho(\vec{r})$, difference between the valence charge density of the defect $\rho(r)$ and that of *x*-Si, $\rho^0(r)$. Notation and units as in Fig. 3.

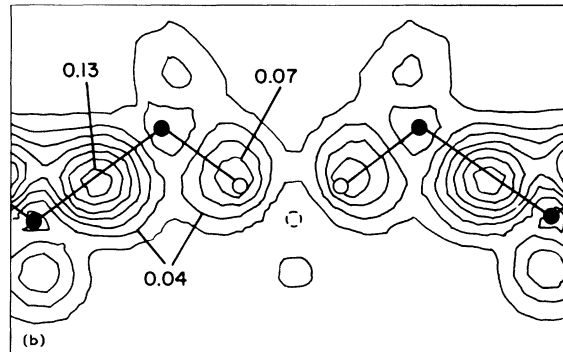
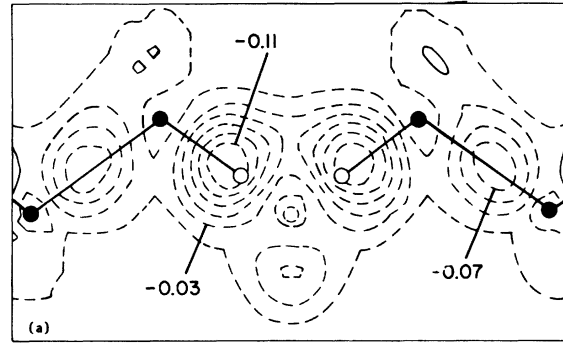


FIG. 5. (a) $\Delta\rho(\vec{r})$ and (b) $\rho(\vec{r})$ of the hydrogenated vacancy for eigenstates in the top 0.25 eV of the valence band. Notation and units as in Fig. 3.

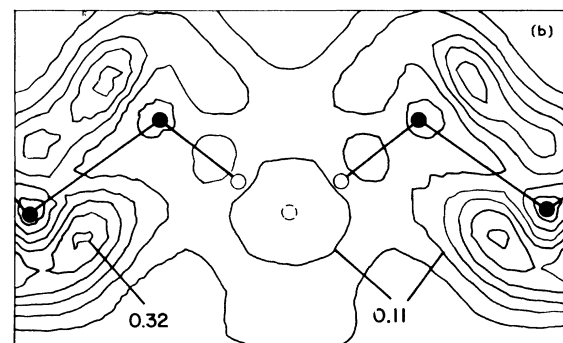
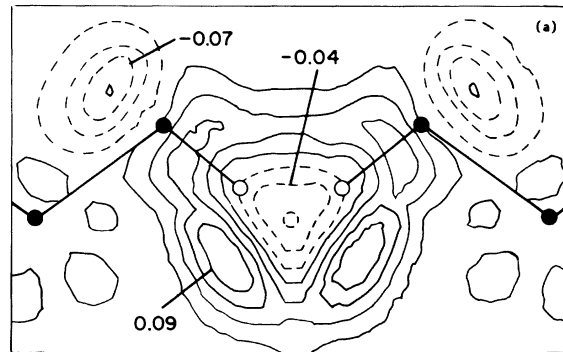


FIG. 6. (a) $\Delta\rho(\vec{r})$ and (b) $\rho(\vec{r})$ of the hydrogenated vacancy for eigenstates in the bottom 0.25 eV of the conduction band. Notation and units as in Fig. 3.

difference density and charge density only for those states within 0.25 eV of the valence-band edge. This result is obtained from Eq. (7) by integrating over the limits -0.25 to 0 eV rather than $-\infty$ to E_F . In contrast to the results for the total valence charge, the Si-H region shows a 70% decrease in charge at the valence-band edge as compared with an undisturbed Si-Si bond in the same energy region. This confirms in real space the picture of the Si-H bond as a repulsive center for band-edge holes. Of perhaps greater significance in Fig. 5 is that this charge disturbance has considerable range: the neighboring Si-Si bond has lost about 30% of its charge at the valence-band edge, and even the next-nearest-neighbor bond has a perceptible charge depletion. We have found that this long-ranged behavior is not unique to the top of the valence band. For example, the charge disturbance at the bottom 0.25 eV of the conduction band (Fig. 6) extends beyond the first-nearest neighbors of the defect. However, the barrier presented to band-edge electrons is qualitatively different from that for band-edge holes. In particular, note that the antibonding conduction-band charge is not peaked on the bonding axes. The region of charge depletion (that is, electron repulsion) is a shell at a radius beyond the first-neighbor Si's while closer to the vacancy, the charge is enhanced in the region around the Si-H bonds.

The nature of the valence-band states changes gradually as we move to energies farther away from the band edge. For about the first 2 eV the picture is essentially the same as the band edge, with depletion of bond charge in the vicinity of the defect. For lower energy this feature rev-

ers, with charge accumulation in the Si-H bond. This accumulation reaches its maximum concentration near -4.5 eV (shown in Fig. 7), corresponding to the pronounced peak in $\Delta N(E)$ near -4.5 eV in Fig. 2. For still lower energies the Si-H bond-charge peak persists down to the bottom of the valence band, but is smaller and more diffuse. The density-of-states peak near -4.5 eV has been seen in most other theoretical calculations of hydrogenated Si (Refs. 4, 7, and 9); Bethe-lattice studies⁷ have established that this structure is the most important result of introducing bonded H in a Si network. A density-of-states peak in this energy range has been found experimentally through photoemission.¹⁴ Other experimental peaks assigned to monohydride configurations¹⁴ are at approximately -7.5 and -10.5 eV. Although our $\Delta N(E)$ contains features near these energies, as have previous density-of-states studies,^{4,7} these peaks result from shifts in the density of states of the perfect sixfold ring structure of the surrounding Si network.⁷ We choose to stop short of a quantitative comparison between our results and photoemission, since it is likely that a variety of H environments are present in *a*-Si:H. For instance the results of Ref. 7 support the assignment of the -4.5 -eV peak to H atoms bonded to adjacent Si's.

We have also calculated the local density of states in

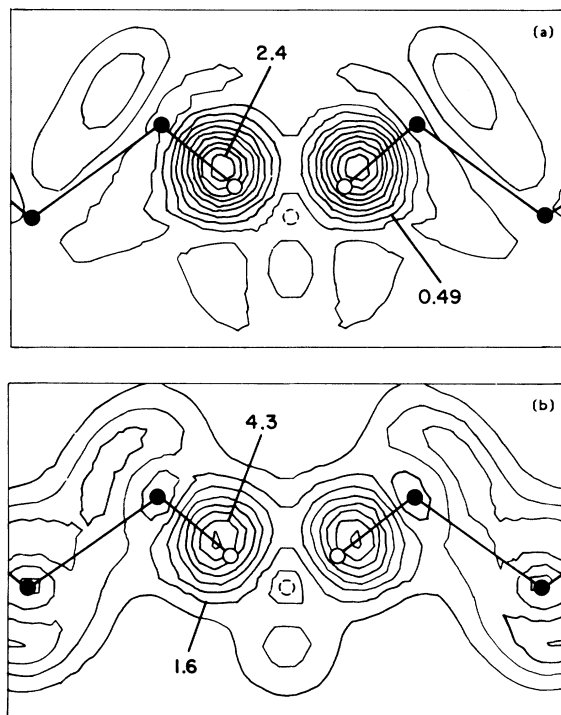


FIG. 7. (a) $\Delta\rho(\vec{r})$ and (b) $\rho(\vec{r})$ of the hydrogenated vacancy for eigenstates between -5 and -4 eV in the valence band. Notation and units as in Fig. 3.

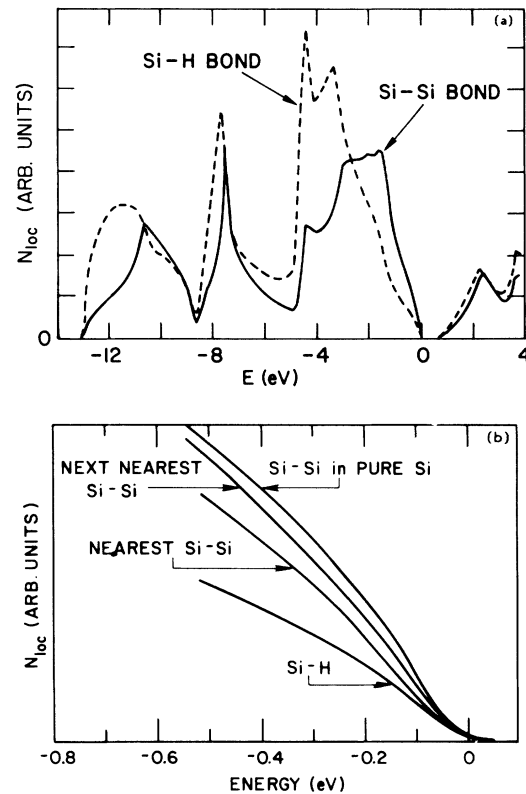


FIG. 8. Local density of states for the region of the Si-H bond (dashed curve) and for an Si-Si bond (solid). On this energy scale all Si-Si bonds are essentially identical. (b) Local density of states at the valence-band edge for an Si-H bond, the nearest Si-Si bond, the next-nearest Si-Si bond, and a remote Si-Si bond.

TABLE II. Parameters for Gaussian fit $V(r) = \sum_i \beta_i e^{-\alpha_i r^{-2}}$, with β_i in Ry and α_i in a.u.⁻².

	α_1	β_1	α_2	β_2	α_3	β_3
$V_{\text{Si}}^{\text{SC}}$	0.633	20.0	0.457	-17.7		
V_{H}^{SC}	1.15	-4.35				
V_{H}^{at}	1.8414	-3.4506	0.4015	-1.0475	0.0543	-0.4079

various regions around the defect. This quantity is given by

$$N_{\text{loc}}(E) = \sum_{\alpha, \alpha'} \int_{\text{bond}} \Phi_{\alpha}^*(\vec{r}) \left[-\frac{2}{\pi} G_{\alpha\alpha'}(E) \right] \Phi_{\alpha'}(\vec{r}) d\vec{r}, \quad (10)$$

where the integral is performed within a sphere centered on various bonds: the Si–H bond, the first-nearest and second-nearest neighbor Si–Si bonds, and a remote Si–Si bond. The results are shown in Fig. 8. All of the local densities projected in this way retain features of the x -Si density of states. The procedure used here to construct the local density of states is different in detail than that used in previous theoretical work.^{4,5,7,9} Still, the general features of $N_{\text{loc}}(E)$ are similar to those found by earlier studies, including (1) the narrowing of the heavy-hole peak in the H-rich region consistent with the reduction of the $pp\pi$ interaction reported in Ref. 4, (2) the general movement of the density of states in the Si-H region to lower energy relative to the Si-Si region, and (3) the recession of the valence-band edge near the defect. However, previous studies have not noted the spatial dependence of the valence-band-edge recession. Figure 8(b) shows this spatial dependence. Measured from the Si–H bond, the recession is significant even as far as the second Si–Si bond. We shall return in the Discussion to the consequences of this long-ranged disturbance caused by the hydrogenated defect.

We emphasize that all of the quantitative results shown above depend on determining a correct self-consistent defect potential. To demonstrate this we have extracted from our results a self-consistent H pseudopotential. This is accomplished by fitting the final potential to a site-centered form

$$V^{\text{SC}}(\vec{r}) = -V_{\text{Si}}^{\text{SC}}(\vec{r}) + \sum_{i=1}^4 V_{\text{H}}^{\text{SC}}(|\vec{r} - \vec{r}_i^{\text{H}}|). \quad (11)$$

We have assumed $V_{\text{Si}}^{\text{SC}}(\vec{r})$ to be the same as in an earlier analysis of the bare Si vacancy³ and therefore have been able to extract $V_{\text{H}}^{\text{SC}}(\vec{r})$. Both $V_{\text{Si}}^{\text{SC}}$ and V_{H}^{SC} have been fitted by a sum of Gaussians: $V^{\text{SC}}(\vec{r}) = \sum_i \beta_i e^{-\alpha_i r^2}$. The values of the fitting constants β_i and α_i are given in Table II. To demonstrate the accuracy of this decomposition, we have recalculated $\Delta N(E) = N(E) - N^0(E)$ using Eqs. (3)–(5), with V in Eqs. (3) and (4) replaced by the fitted V^{SC} of Eq. (11). As Fig. 9 shows, $\Delta N(E)$ computed in this manner agrees very well with the actual self-consistent $\Delta N(E)$. This demonstrates that the defect potential can be decom-

posed into site-centered contributions. However, there are substantial differences between V_{H}^{SC} and the potential of an isolated H atom V_{H}^{at} . (We have also fitted V_{H}^{at} by a sum of Gaussians; see Table II.) While V_{H}^{at} and V_{H}^{SC} are quite similar near the origin, the long tail of the atomic potential is absent in V_{H}^{SC} because of the screening effect of its Si environment. Consequently the integrated strength of the self-consistent H potential is smaller than the atomic potential by a factor of 10. It is clear that a non-self-consistent calculation based on the superposition of atomic potentials would have given very poor results.

V. DISCUSSION

In the preceding sections we have presented detailed results for the electronic structure of a particular model hydrogenated site in crystal Si. We now use these results to make several estimates which are relevant to the transport and optical properties of a -Si:H. We propose that the quantum-well model provides a link between the present calculation and this goal. The model⁶ assumes that the presence of H is the dominant disorder for the band-edge properties of a -Si:H, of greater importance, for example, than oddfold Si rings or dihedral-angle distortions.^{16,17} It further assumes that the individual hydrogenated defects create disturbances which extend $\sim 1\frac{1}{2}$ bond lengths from the vacancy site into the Si network. This implies that defects do not interact strongly enough to form a pseudo-binary alloy, but that each disturbance by itself has sufficient extent to isolate regions of pure Si. Within these as-

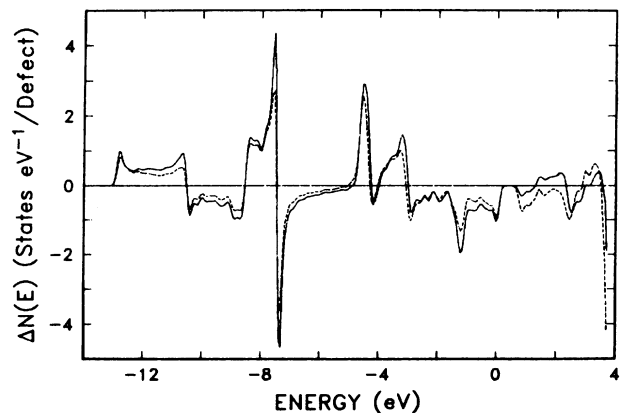


FIG. 9. $\Delta N(E)$ for the hydrogenated vacancy calculated using the fully-self-consistent potential (solid line) and using the sum of site-centered Si and H potentials as in Eq. (11) (dashed line).

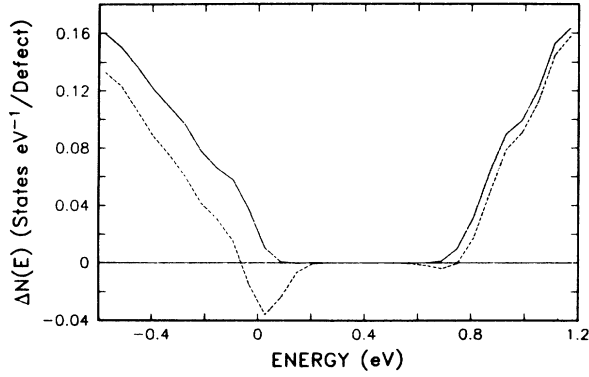


FIG. 10. Approximate density of states $N(E)$ for a -Si:H for a defect concentration of $f=0.05$.

sumptions, the local information obtained from our Green's-function calculation can be transferred to the quantum-well model. We now show that this transfer provides support for many of the predictions of the quantum-well model. Keep in mind, however, that the estimates which we will now give do not have the rigor of the results of the Green's-function calculation for the model defect given above.

To illustrate a simple procedure for transferring our single-defect results into the many-defect solid (a -Si:H), we consider an elementary picture of a mixture of a Si with a Si_4H_4 system, the latter being the composition of a defect site. We assume the individual hydrogenated defects to be noninteracting. Under this condition, the density of states is just $N(E) = N^0(E) + f \Delta N(E)$, where $N^0(E)$ is the Si density of states, $\Delta N(E)$ is the change in the density of states from a single defect (Fig. 2), and f is the defect concentration. This construction of $N(E)$ is similar in spirit but much more approximate than the coherent-potential-approximation approach used in Ref. 4. Since each defect contains four hydrogens, the hydrogen concentration [H] is $4f$. Such a $N(E)$ is shown in Fig. 10 for $f=0.05$ along with $N^0(E)$. The nature of our estimate for $N(E)$ produces grossly nonphysical features, such as a negative density of states at each band edge. This is a result of neglecting the interactions between neighboring defect sites, and Fig. 10 suggests that such interactions are most important near the band gap. Still, the overall picture is correct: The band edges recede with the introduction of H. In order to examine the shift of the band edges with H concentration, we have studied the following measure of the new band edges $E_{v,c}^f$:

$$\int_{E_{v,c}^0}^{E_{v,c}^f} N(E) dE = 0. \quad (12)$$

So in a very approximate way we attempt to average the negative density near the old band edge with the adjoining positive density. Figure 11 shows the new valence- and conduction-band edges E_v^f and E_c^f as a function of f , as estimated by Eq. (12). For $f=0.05$ the relative increase of the band gap is significantly smaller than experiment.¹⁸ Disorder effects not included in this simple model, e.g., localization, cause additional widening of measurable gaps⁴ in real films. Figure 11 agrees with the theoretical esti-

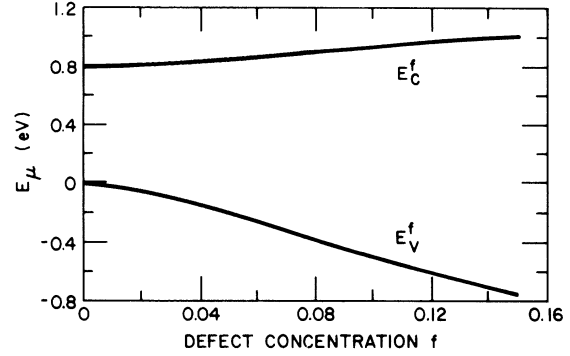


FIG. 11. Energies of the valence and conduction bands E_v^f and E_c^f as estimated by Eq. (12) as a function of defect concentration f .

mate of the overall band-gap widening due to H disorder in Ref. 4, although we disagree on how much of this widening occurs at each band edge. While both the present work and Ref. 4 find that the effect is largest at the valence-band edge, Fig. 11 shows a small recession of the conduction-band edge. Reference 4 finds no such effect.

The above simple picture, while useful for obtaining a rough estimate of the band-gap expansion due to a finite number of H defects in the Si host, is incapable of predicting the localization properties of the eigenstates in a -Si:H. As discussed above, the Green's-function calculation provides detailed information about the effect of the disturbance on the eigenstates, apart from simply the change in the density of states $\Delta N(E)$. We can use this additional information to make some estimates of band-edge localization and thereby test some of the assumptions and predictions of the quantum-well model. One of the initial premises of the model was that the presence of a Si-H bond excluded band-edge carriers, both electrons and holes, from its vicinity out to a range of about 1.5 bond lengths. If we identify the exclusion of carriers with the removal of charge density around the defect, then Figs. 5 and 6 provide the information to test this assumption. As discussed above, Fig. 5 shows that there is a substantial removal of charge from the Si-H bond as compared with a Si-Si bond near the valence-band edge. At the conduction-band edge, Fig. 6 shows a slight addition of charge near the Si-H bonds, and a removal of charge at the Si sites, resulting in a net removal of charge (Fig. 2). To this extent two assumptions of the quantum-well model are confirmed. Moreover, the Green's-function calculations provide the necessary information about the range of this charge removal. The range of the band-edge disturbances is seen to be beyond the Si-H bond itself. To quantify this range for the valence-band edge, we have looked at the envelope of the charge disturbance $\Delta\rho(r)$ (Fig. 5), averaging out the rapid variation in the bond region. We find that this smoothed quantity can be fitted by an exponential decay

$$\Delta\rho(r) = \rho^0(r) e^{-r/r_c}. \quad (13)$$

The mean decay length $r_c = 2.7 \text{ \AA}$, measured from the center of the vacancy, is well into the first Si-Si bond.

By this measure the additional assumption of the quantum-well model that the range of the disturbance caused by the Si-H bond must extend, on the average, halfway into the adjoining Si-Si bond, is confirmed for the valence-band edge.

It is important to illustrate that the assumed formation of localized states in regions of pure Si is dependent on the range of the defect as well as its magnitude. Reference 6 used a two-dimensional square lattice to illustrate the range dependence. To improve on this, we have studied the percolation properties of a three-dimensional, fourfold-coordinated diamond lattice with removed sites of varying range. By numerical simulation on an 8000-atom lattice, we have computed the percolation threshold, that is, the concentration of removed sites needed to block all the classical paths connecting one end of the sample to the other. These simulations confirm the empirical criterion for percolation¹⁹ which states that all bond paths will be cut off if more than $x_c = 0.85$ of the volume is removed. This criterion is embodied by the following relation between the range of the defect r_c and the defect concentration f :

$$\frac{4}{3} \pi r_c^3 = \frac{-\Omega_{\text{Si}}}{f} \ln \left(\frac{1-x_c}{\eta} \right). \quad (14)$$

Here $\Omega_{\text{Si}} = 20 \text{ \AA}^3$ is the average volume per Si atom and $\eta = 0.34$ is the diamond-lattice hard-sphere packing fraction. Table III gives the results of Eq. (14) for various defect concentrations. The absence of classical bond paths suggests but does not prove the existence of the localized states; for valence-band states, whose charge density follows the bonds in the solid, the results are most applicable. As we have demonstrated above, the range of the disturbance at the valence-band edge is between one and two bond lengths. Table III shows that for this range between a 25 and 15 at. % concentration of defects is needed to stop percolation. Typically $[H] = 15-20$ at. % in *a*-Si:H. The relevant measured concentration of isolated Si-H bonds is 5% to which must be added some fraction of the total $[H]$ that is in clusters.²⁰ Each cluster acts essentially as a larger single Si-H defect. So, the measured defect concentrations are in the range necessary to cut off percolation at the valence-band edge.

Unfortunately the connection between the classical percolation limits and the position of the mobility edges is at best qualitative. For example, in the classical picture all states are either extended (percolating) or localized, while in a quantum-mechanical description some states are localized no matter how small the potential disturbance.

TABLE III. Defect range required to cut off percolation.

Required range r_c (Å)	Defect concentration f (at. %)
2.5	25
2.7	20
3.0	15
3.4	10
4.3	5

Therefore we have attempted to make some simple quantum estimates of localization in the hydrogenated Si system. A very elementary model based on the Anderson criterion for localization²¹ gives the simple and intuitively appealing result (see Appendix for derivation),

$$E_\mu \cong [H] |E_H - E_{\text{Si}}|. \quad (15)$$

Here E_μ is the energy width of localized states (i.e., the difference between the mobility and band edges), and E_H and E_{Si} are characteristic energies of the H and Si subsystems. Thus, the localization is directly proportional to the defect concentration and to the energy mismatch between the defect and the bulk. We obtain a value for E_μ from Eq. (15) by estimating E_H and E_{Si} for the valence band from the average shifts of the local densities of states in Fig. 8(a). Taking either the shift of the band edge, of the main peak in the density of states, or of the entire valence band, we estimate $|E_H - E_{\text{Si}}| \sim 1$ eV. A previous estimate^{4,14} has given $|E_H - E_{\text{Si}}| \sim 0.4$ eV. Taking $[H] = 5-15$ at. % gives $E_\mu = 0.05-0.15$ eV for the valence-band edge. This rather small estimate for E_μ is not surprising considering the inaccuracies of this simple application of the Anderson localization model, i.e., the tight-binding approximation, the constancy of off-diagonal matrix elements, and the failure to account for the reduced coordination of H (1) as compared with Si (4). As discussed in the Appendix all these effects increase localization. So Eq. (15), while providing an appealing intuitive picture of the effects which lead to localization, is not quantitatively reliable within the context of the approximations available.

We can, however, perform a different type of quantum-mechanical estimate of localization which, while still not rigorously justifiable, is directly comparable to the estimates which have been previously made for dihedral-angle disorder in *a*-Si.¹⁶ We can therefore compare the relative importance of H-induced versus network-induced disorder in *a*-Si:H.

In Ref. 16, Yonezawa and Cohen estimated the effect of dihedral-angle disorder on localization in *a*-Si by using the following formula for the position of the mobility edge:

$$E_\mu = \bar{E}_b = \frac{1}{\Omega} \int E_b(\vec{r}) d\vec{r}, \quad (16)$$

where $E_b(\vec{r})$ is the local value of the band edge in the disordered system. To apply Eq. (16) to the H-disordered system, one must estimate the local band edge near the H defect in *a*-Si:H. As a first step in performing this estimate we use a simplified effective-mass description of the Si conduction- and valence-band edges. The conduction-band edge is represented by six noninteracting valleys each with effective mass $m_c = 0.32m_0$ [$= (m_e^*)^{1/3} (m_t^*)^{2/3}$, $m_e^* = 0.92m_0$, $m_t^* = 0.19m_0$],²² and the valence-band edge by three parabolic noninteracting bands at Γ with effective masses $m_{v1}^* = 0.49m_0$, $m_{v2}^* = 0.16m_0$, and $m_{v3}^* = 0.245m_0$.²³ Within this representation we have constructed spherically symmetric model potentials which reproduce the integral of $\Delta N(E)$ (Fig. 2) within 0.5 eV of the band edges. We have chosen these model potentials to be Gaussians,²⁴

$$V(\vec{r}) = ue^{-r^2/r_c^2}, \quad (17)$$

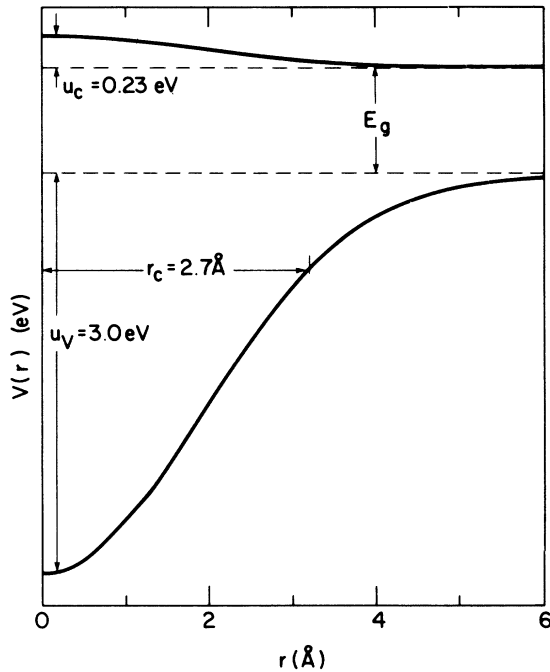


FIG. 12. Model potentials for the conduction- and valence-band edges which mimic the effect of the real hydrogenated vacancy on the density of states $\Delta N(E)$ (see Fig. 2). Within the effective-mass theory these model potentials may be viewed as local band edges, as drawn.

with the same decay length as the calculated change in charge density $\Delta\rho(r)$ [Eq. (13)], i.e., $r_c = 2.7 \text{ \AA}$. For this r_c we find that the parameters $u_v = 3.0 \text{ eV}$ and $u_c = 0.23 \text{ eV}$ accurately reproduce the $\Delta N(E)$ for the valence- and conduction-band edge, respectively. Within the Thomas-Fermi model of electron dynamics $V(\vec{r})$ has more significance than just a model potential. In fact we interpret it as the local band edge $E_b(\vec{r})$ (see Fig. 12),²⁵ just the quantity we need to apply Eq. (16) for the mobility edge. Substituting Eq. (17) into Eq. (16),

$$E_\mu = \frac{f}{\Omega_{\text{Si}}} \pi^{3/2} u r_c^3. \quad (18)$$

The identification of $V(\vec{r})$ with a local band edge is justified under the condition $u r_c^2 \gtrsim 1 \text{ a.u.} = 7.6 \text{ eV \AA}^2$. This condition is satisfied for the model potentials which we have constructed. From Eq. (18) we obtain the following estimates of the mobility edges: $E_v = 0.8 \text{ eV}$ and $E_c = 0.06 \text{ eV}$. These results are quite insensitive to the choice of parameters $u_{v,c}$ and r_c as long as the resulting potential reproduces $\Delta N(E)$ at the band edges. Note that as before, the effect of H on the valence-band edge is predicted to be much greater than at the conduction-band edge. As for the relative importance of H-induced disorder, the present value of $E_\mu = 0.8 \text{ eV}$ when compared with the estimated $E_\mu = 0.3 \text{ eV}$ for dihedral-angle disorder¹⁶ suggests that the presence of H has a greater effect than intrinsic Si network defects on valence-band eigenstates.

VI. CONCLUSIONS

We have calculated the electronic structure of the H-saturated monovacancy in x -Si. No gap states are introduced by the defect, and states are removed from the top of the valence band. This is in agreement with the traditional understanding of the role of H in a -Si:H. We also find a slight removal of states from the bottom of the conduction band. The defect eigenstates at the edge of the conduction band are enhanced near the Si-H bonds and reduced near the removed Si site. The eigenstates at the edge of the valence band behave quite differently, with reduced density in the Si-H bonds and in the neighboring Si-Si bonds. Both the valence- and conduction-band edge eigenstates are correctly described as "barriers" to the passage of band-edge carriers through the H-rich region. This is consistent with the assumptions of the quantum-well model.

We have studied a number of simple models for band-edge localization resulting from H disorder. We have obtained estimates for the region of localized states of 0.05–0.8 eV for the valence band of 0.01–0.06 eV for the conduction band. The variability of these estimates reflects the lack of any rigorous theory for the position of the mobility edges. We are able to determine that the effect of H disorder is greater than that of dihedral-angle disorder at the valence-band edge, and the effect of H is much greater at the valence- than at the conduction-band edge.

ACKNOWLEDGMENTS

We thank N. O. Lipari, Z. Levine, S. T. Pantelides, and A. R. Williams for several useful discussions. This work

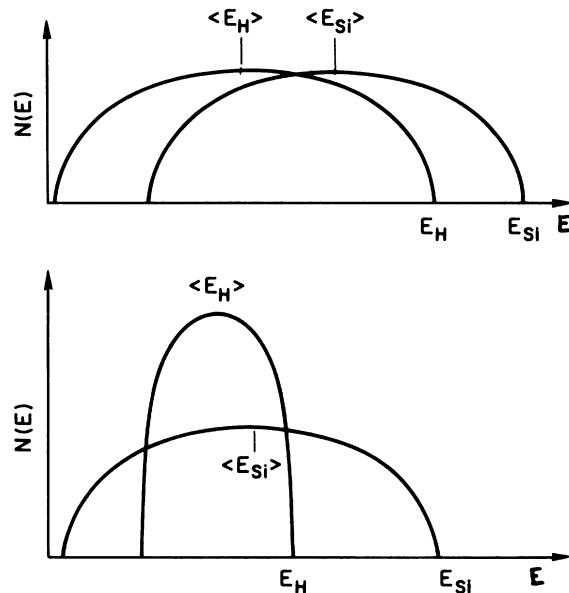


FIG. 13. Schematic illustration of how ignoring the narrow bandwidth of the H-rich component of a Si-H alloy can lead to underestimates of the band-edge effects if $\langle E_H \rangle - \langle E_{\text{Si}} \rangle$ rather than $E_H - E_{\text{Si}}$ is used in Eq. (A4). Top panel shows the density of states of a hypothetical Si + H system in which V is constant; the bottom panel is a more realistic representation in which V is smaller in the extreme H-rich limit.

was supported in part by the Solar Energy Research Institute (SERI) under Subcontract No. ZZ-0-9319 and by the National Science Foundation—Materials Research Laboratory program under Grant No. DMR-79-23647.

APPENDIX

In this Appendix we show how Eq. (15) in the text is obtained using the Anderson criterion for localization. In the Anderson approach we assume that a minimal tight-binding description of the disordered Si + SiH system exists with a constant off-diagonal matrix element V and diagonal matrix elements for Si and SiH, E_{Si} and E_{H} . Then the quantity which gives information about localization is²⁶

$$S(E) = z \exp \left[\int \ln \left| \frac{V}{E - E'} \right| P(E') dE' \right], \quad (\text{A1})$$

where z is the average coordination number of the solid and $P(E)$ is the probability distribution of diagonal matrix elements, which for a system with randomly dispersed H's is

$$P(E) = [\text{H}] \delta(E - E_{\text{H}}) + (1 - [\text{H}]) \delta(E - E_{\text{Si}}), \quad (\text{A2})$$

where $[\text{H}]$ is the hydrogen concentration.

$S(E)$ predicts the presence of localized states at energy E according to the rule

$$\begin{aligned} S(E) &> 1 \quad \text{for extended states,} \\ S(E) &< 1 \quad \text{for localized states,} \\ S(E_{\mu}) &= 1 \quad \text{for mobility edge.} \end{aligned} \quad (\text{A3})$$

If we assume $[\text{H}] \ll 1$ and E_{μ} much less than the valence-band width, Taylor-series expansion of Eq. (A1) gives the simple result

$$E_{\mu} \cong [\text{H}] | E_{\text{H}} - E_{\text{Si}} |, \quad (\text{A4})$$

which is Eq. (15) in the text. The above analysis contains a number of gross approximations: The simple assumed tight-binding model, the constancy of the hopping matrix element V , and the constancy of the coordination number z . Doubtless V is smaller in the H-rich region and, as shown in Fig. 13, leads to an underestimate of $E_{\text{H}} - E_{\text{Si}}$ in Eq. (A3). Thus Eq. (A3) should only be taken as a qualitative prediction of the mobility edge, in particular with respect to the meaning of the energy difference between the alloy constituents.

¹Proceedings of the 9th International Conference on Amorphous and Liquid Semiconductors, Grenoble, France, 1981, edited by B. K. Chakraverty and D. Kaplan, [J. Phys. (Paris) Colloq. **42**, C4 (1981)].

²Preliminary accounts of this work were given in D. P. DiVincenzo, J. Bernholc, and M. H. Brodsky, J. Phys. (Paris) Colloq. **42**, C4-137 (1981); D. P. DiVincenzo, J. Bernholc, M. H. Brodsky, N. O. Lipari, and S. T. Pantelides, in *Tetrahedrally Bonded Amorphous Semiconductors, Carefree, Arizona*, A Topical Conference on Tetrahedrally Bonded Amorphous Semiconductors, edited by R. A. Street, D. K. Biegelson, and J. C. Knights (AIP, New York, 1981), p. 156.

³J. Bernholc, N. O. Lipari, and S. T. Pantelides, Phys. Rev. B **21**, 3545 (1980).

⁴D. A. Papaconstantopoulos and E. N. Economou, Phys. Rev. B **24**, 7233 (1981); in *Tetrahedrally Bonded Amorphous Semiconductors*, Ref. 2, p. 130; E. N. Economou and D. A. Papaconstantopoulos, Phys. Rev. B **23**, 2042 (1981).

⁵W. E. Pickett, Phys. Rev. B **23**, 6603 (1981); **26**, 5650 (1982).

⁶M. H. Brodsky, Solid State Commun. **36**, 55 (1980).

⁷D. C. Allan, J. D. Joannopoulos, and W. B. Pollard, Phys. Rev. B **25**, 1065 (1982); D. C. Allan and J. D. Joannopoulos, Phys. Rev. Lett. **44**, 43 (1980).

⁸K. H. Johnson, H. J. Kolari, J. P. de Neufville, and D. L. Morel, Phys. Rev. B **21**, 643 (1980).

⁹W. Y. Ching, D. J. Lam, and C. C. Lin, Phys. Rev. Lett. **42**, 805 (1979); Phys. Rev. B **21**, 2378 (1980).

¹⁰Using information from infrared spectra of *a*-Si:H and of substituted silane molecules, Lucovsky [G. Lucovsky, Solid State Commun. **29**, 571 (1979)] has inferred a Si-H bond length of 1.52 Å. We do not believe that this small change in the bond length would qualitatively change any of the results of our calculation.

¹¹J. Bernholc, N. O. Lipari, S. T. Pantelides, and M. Sheffler,

Phys. Rev. B **26**, 5706 (1982).

¹²G. F. Koster and J. C. Slater, Phys. Rev. **96**, 1208 (1954).

¹³W. Kohn and L. J. Sham, Phys. Rev. **140**, A1133 (1965).

¹⁴B. von Rödern, L. Ley, M. Cardona, and F. W. Smith, Philos. Mag. B **40**, 433 (1979).

¹⁵J. A. Appelbaum and D. R. Hamann, Phys. Rev. Lett. **34**, 806 (1975); K. M. Ho, M. L. Cohen, and M. Schlüter, Phys. Rev. B **15**, 3888 (1977).

¹⁶F. Yonezawa and M. H. Cohen, in *Fundamental Physics of Amorphous Semiconductors*, edited by F. Yonezawa (Springer, Berlin, 1981), p. 119.

¹⁷J. H. Davies, Philos. Mag. B **41**, 373 (1980).

¹⁸The crystal Si band gap of $E_G = 0.8$ eV in the present calculation is a well-known artifact of the local-density approximation.

¹⁹H. Scher and R. Zallen, J. Chem. Phys. **53**, 3759 (1973).

²⁰J. A. Reimer, R. W. Vaughan, and J. C. Knights, Phys. Rev. Lett. **44**, 1936 (1981). We believe that although the model defect which we use in our calculation contains four H atoms, the range of the disturbance caused by this defect is representative of a single monohydride unit, since this range is much greater than that of the Si-H unit itself. Thus we make a one-to-one correspondence between f and $[\text{H}]$, except when H occurs in clusters.

²¹P. W. Anderson, Phys. Rev. **109**, 1492 (1958).

²²J. C. Hensel, H. Hasegawa, and M. Nakayama, Phys. Rev. **138**, A225 (1965).

²³R. A. Smith, *Semiconductors* (Cambridge University Press, Cambridge, 1959), p. 350.

²⁴In the rigorous effective-mass theory the defect potential should be the same for both the conduction- and valence-band edges and should also be equal to the actual defect potential of Eq. (7). However, we have made various approximations to the rigorous effective-mass description of the Si band edges,

i.e., neglect of intervalley coupling, of conduction-band anisotropy, and of heavy-hole—light-hole coupling. Therefore we have permitted the conduction- and valence-band defect potentials to be different from Eq. (7) and from each other so that a particular physical property of the actual defect, $\Delta N(E)$

at the band edges, is reproduced.

²⁵J. M. Ziman, *Models of Disorder* (Cambridge University Press, Cambridge, 1979), p. 483.

²⁶J. M. Ziman, *Models of Disorder*, Ref. 25, Chap. 9.